

Characterization of the inositol phosphorylceramide synthase activity from *Trypanosoma cruzi*

Juliana M. FIGUEIREDO, Wagner B. DIAS, Lucia MENDONÇA-PREVIATO, José O. PREVIATO and Norton HEISE¹

Instituto de Biofísica Carlos Chagas Filho (IBCCF), Centro de Ciências da Saúde (CCS) Bloco G, Universidade Federal do Rio de Janeiro (UFRJ), Cidade Universitária, Ilha do Fundão, Rio de Janeiro-RJ, 21944-970, Brazil

IPC (inositol phosphorylceramide) synthase is an enzyme essential for fungal viability, and it is the target of potent antifungal compounds such as rustmicin and aureobasidin A. Similar to fungi and some other lower eukaryotes, the protozoan parasite *Trypanosoma cruzi* is capable of synthesizing free or protein-linked glycoinositolphospholipids containing IPC. As a first step towards understanding the importance and mechanism of IPC synthesis in *T. cruzi*, we investigated the effects of rustmicin and aureobasidin A on the proliferation of different life-cycle stages of the parasite. The compounds did not interfere with the axenic growth of epimastigotes, but aureobasidin A decreased the release of trypomastigotes from infected murine peritoneal macrophages and the number of intracellular amastigotes in a dose-dependent manner. We have demonstrated for the first time that all forms of *T. cruzi* express an IPC synthase activity that is capable of transferring inositol phosphate from phosphatidylinositol to the C-1 hydroxy group of C₆-NBD-cer {6-[N-(7-nitro-2,1,3-benzoxadiazol-4-yl)-

amino]hexanoylceramide} to form inositol phosphoryl-C₆-NBD-cer, which was purified and characterized by its chromatographic behaviour on TLC and HPLC, sensitivity to phosphatidylinositol-specific phospholipase C and resistance to mild alkaline hydrolysis. Unlike the *Saccharomyces cerevisiae* IPC synthase, the *T. cruzi* enzyme is stimulated by Triton X-100 but not by bivalent cations, CHAPS or fatty-acid-free BSA, and it is not inhibited by rustmicin or aureobasidin A, or the two in combination. Further studies showed that aureobasidin A has effects on macrophages independent of the infecting *T. cruzi* cells. These results suggest that *T. cruzi* synthesizes its own IPC, but by a mechanism that is not affected by rustmicin and aureobasidin A.

Key words: aureobasidin A, Chagas disease, glycoinositolphospholipid (GIPL), inositol phosphorylceramide (IPC) synthase, sphingolipid synthesis, *Trypanosoma cruzi*.

INTRODUCTION

The protozoan parasite *Trypanosoma cruzi* is the causative agent of Chagas disease (American trypanosomiasis), an incurable infection affecting millions of people in Latin and Central America. Through a co-ordinated multi-country programme, the transmission of Chagas disease through insects and blood transfusion has been controlled in several endemic areas, with average decrease in incidence 94 % between 1994 and 2000 [1]. However, 21 000 deaths and 200 000 new cases are still reported annually in 15 Southern Cone countries [1]. In all life-cycle stages of *T. cruzi* [2], most of its surface glycoconjugates are attached to the plasma membrane through a GPI (glycosylphosphatidylinositol) anchor [3]. These components may include GPI-anchored proteins and GIPLs (glycoinositolphospholipids), which are free glycolipids comprising an inositol phospholipid and a short glycan chain similar to protein-linked GPI anchors, where the motif Man- α -(1 \rightarrow 4)GlcN- α -(1 \rightarrow 6)*myo*-inositol phosphate is conserved [4,5].

It has been suggested that GPI-anchored surface components such as the 1G7-antigen, gp82, *trans*-sialidase, mucin-like glycoproteins and GIPLs are essential for invasion and intracellular survival of the parasite in mammalian host cells [3,6]. For example, mucin-like glycoproteins, which are the only sialic acid acceptors on the surface of the parasite, are released during the entry into mammalian cells, whereas the 1G7-antigen is not [7]. The fact that, in epimastigotes, the lipid domain of the mucin GPI anchor [8,9] is an alkyl-acyl-glycerol as in the 1G7-antigen anchor

[10], whereas, in infective metacyclic trypomastigotes, the mucins are mostly anchored through IPC (inositol phosphorylceramide) suggests that the heterogeneous lipid portions between these two molecules might play a role in the differential release during the infection process [7,9]. Consequently, delineation of *T. cruzi*-specific GPI metabolic pathways could disclose potential targets for chemotherapy of the Chagas disease.

GPI anchors are assembled in the endoplasmic reticulum by sequential transfer of monosaccharides and EtNP (ethanolamine phosphate) to PI (phosphatidylinositol), forming the minimal precursor structure EtNP-Man₃-GlcN-PI [4]. Although we have previously shown that *T. cruzi* GPI-protein anchors are assembled in the same way as a minimal GPI precursor, their structures differ, being composed of a Man-(EtNP)-Man₃-GlcN-PI in which an aminoethylphosphonate may replace EtNP and a further aminoethylphosphonate can be linked to GlcN [11]. All proposed schemes for GPI biosynthesis postulate endogenous PI as initial acceptor. Subsequent sugar-transfer reactions are fairly well characterized and have been recently validated as the drug target for African trypanosomiasis or sleeping sickness [12]. However, less attention has been paid to the source of the initial PI species. Studies in *Leishmania mexicana* identified two major PI pools with distinctive alkyl-chain compositions for the biosynthesis of protein and lipophosphoglycan anchors [13]. In contrast with *L. mexicana*, the ether-lipid chains for all protein GPI anchors [7–10,14–16] and GIPLs [17] so far described in *T. cruzi* are mostly *sn*-1-*O*-hexadecyl-2-*O*-acyl-glycerol. In addition, GIPLs

Abbreviations used: BHI, brain-heart infusion; C₆-NBD-cer, 6-[N-(7-nitro-2,1,3-benzoxadiazol-4-yl)amino]hexanoylceramide; DTT, dithiothreitol; EtNP, ethanolamine phosphate; FCS, foetal calf serum; GIPL, glycoinositolphospholipid; GPI, glycosylphosphatidylinositol; IFN- γ , interferon- γ ; IPC, inositol phosphorylceramide; IP-C₆-NBD-cer, inositol phosphoryl-C₆-NBD-cer; LPS, lipopolysaccharide; M ϕ , murine peritoneal macrophages; PC, phosphatidylcholine; PE, phosphatidylethanolamine; PI, phosphatidylinositol; PI-PLC, PI-specific phospholipase C from *Bacillus thuringiensis*; SBP, sphingolipid biosynthetic pathway; TCT, tissue-culture-derived trypomastigote; TX-100, Triton X-100; WT, wild-type.

¹ To whom correspondence should be addressed (email nheise@biof.ufrj.br).

and protein GPI anchors of *T. cruzi* also exist in ceramide-linked forms, composed of dihydrosphingosine long-chain base N-acylated by palmitic (C_{16:0}) or lignoceric (C_{24:0}) acids [9,10,18–23]. The fact that mucin-like molecules, 1G7-antigen [9,10] and GPIs [17] have heterogeneous lipid anchors might imply at least two separate PI pools for anchor biosynthesis, one containing ceramide and the other containing hexadecylglycerol [11]. Alternatively, there could be a remodelling process similar to that observed in some yeast GPI-anchored proteins [24–26] and IPC [27] of *Saccharomyces cerevisiae*.

The major differences in the sphingolipid structure of mammals and fungi are the type of ceramide and the nature of the polar head. In mammals, the ceramide is sphingosine and the head group is phosphocholine [28] or carbohydrate [29], whereas, in fungi, inositol phosphate is transferred to the C-1 hydroxy group of phytoceramide to form IPC, a reaction catalysed by IPC synthase [30]. Although IPC represents a low proportion of fungal phospholipids, they are essential for viability, and the SBP (sphingolipid biosynthetic pathway) has been suggested as a target for antifungal chemotherapy [30,31]. Mutants of *S. cerevisiae* that do not synthesize sphingolipids are not viable, and pathogenic fungi are killed when treated with inhibitors of SBP, particularly those directed against the IPC synthase activity, such as khafrefungin, rustmicin and aureobasidin A [32–35]. Moreover, it has been shown recently that the modulation of IPC synthase activity regulates Pkc1 (fungi homologue of protein kinase C) through bioactive molecules, which are crucial for the activation of virulence factors that contribute in the pathogenesis of *Cryptococcus neoformans* [36,37].

Given the biological importance of sphingo- and ether-lipids to *T. cruzi*, the pathways of PI-containing lipid synthesis, sorting and subsequent lipid-remodelling processes may constitute putative drug targets. Any block in the synthesis of these lipids would impair the expression of millions of GPI-anchored surface glycoconjugates, which could render the parasite less capable of evading the host immune responses or, eventually, render them incapable of dividing or infecting and surviving inside host cells.

In the present study, we have observed that the fungicides rustmicin and aureobasidin A, which are inhibitors of fungal IPC synthase, do not interfere with the growth of epimastigotes of *T. cruzi* in culture. However, aureobasidin A does inhibit, in a dose-dependent manner, both the proliferation of amastigotes inside macrophages and the release of trypomastigotes from these cells. Also, we have identified and characterized for the first time the IPC synthase of *T. cruzi*, and compared its activity with that from yeast. Although present in microsomal membranes of all stages of the parasite, the IPC synthase is not inhibited by rustmicin, aureobasidin A or a combination of both. The results suggest that, in contrast with fungi, the toxicity of aureobasidin A to intracellular forms of *T. cruzi* is not mediated by an inhibition of the biosynthesis of IPC.

EXPERIMENTAL

Materials

Rustmicin was kindly provided by Dr S. Mandala (Merck Research Laboratories, Rahway, NJ, U.S.A.). Aureobasidin A and C₆-NBD-cer {6-[N-(7-nitro-2,1,3-benzoxadiazol-4-yl)amino]-hexanoylceramide} were purchased from Panvera (Madison, WI, U.S.A.) and Molecular Probes (Madison, WI, U.S.A.) respectively. Soya-bean PI, PC (phosphatidylcholine), PE (phosphatidylethanolamine), DTT (dithiothreitol), EDTA, EGTA, PMSF, leupeptin, soya-bean trypsin inhibitor, TX-100 (Triton X-100), CHAPS, fatty-acid-free BSA, zymosan, verapamil and LPS (lipopolysaccharide) from *Escherichia coli* O111:B4 were from

Sigma (St. Louis, MO, U.S.A.). Recombinant murine IFN- γ (interferon- γ) was purchased from Pharmingen (San Diego, CA, U.S.A.). PI-PLC (PI-specific phospholipase C from *Bacillus thuringiensis*) was kindly provided by Dr M. L. Cardoso de Almeida (Universidade Federal de São Paulo, São Paulo, SP, Brazil).

T. cruzi, *C. neoformans*, *Aspergillus fumigatus* and *S. cerevisiae*

T. cruzi (Y strain) was obtained from the Fundação Oswaldo Cruz (Fiocruz, Rio de Janeiro, RJ, Brazil) culture collection. Epimastigotes were axenically cultured in BHI (brain–heart infusion) supplemented with 10 mg · l⁻¹ haemin and 5% (v/v) heat-inactivated FCS (foetal calf serum; BHI-FCS medium) at 28 °C with shaking (~80 rev · min⁻¹) as described before [38]. The cultures were used for evaluating the effects of rustmicin and aureobasidin A on the proliferation of epimastigotes or as source of parasites for the preparation of microsomal membranes.

Bloodstream trypomastigotes obtained after heart puncture of infected Balb/c mice were separated by differential centrifugation and used for the infection of confluent monolayers of Vero cells in culture to establish the intracellular cycle, and maintained in RPMI 1640 medium containing 10% (v/v) FCS under an atmosphere of 5% CO₂ at 37 °C [39]. TCTs (tissue-culture-derived trypomastigotes) were then used to infect LLCMK₂ cells to obtain large quantities of amastigotes or trypomastigotes for the preparation of their microsomal fractions or used to infect *in vitro* murine peritoneal macrophages.

An encapsulated form of *C. neoformans* [strain 444, designated here as WT (wild-type)], originally isolated from a patient with AIDS who developed cryptococcal meningitis, was provided by Professor L. R. Travassos (Universidade Federal de São Paulo), and an acapsular mutant (Cap67) [40] was kindly provided by Dr R. Cherniak (Georgia State University, Atlanta, GA, U.S.A.). Stock cultures were grown on Sabouraud dextrose agar medium at 37 °C for 24 h and maintained at 4 °C. For dose-dependent growth inhibitions, yeast forms were grown in a defined liquid medium at 37 °C in a shaker (~100 rev · min⁻¹) [41]. After 5 days, cells were collected by centrifugation (7000 g, 15 min, 4 °C), washed three times with cold 150 mM NaCl (pH 7.4) and transferred to BHI-FCS medium containing a serial dilution of rustmicin, aureobasidin A or methanol.

A. fumigatus (strain NCPF 2109) was isolated from a patient with aspergillosis at the Mycology Reference Laboratory (Bristol Public Health Laboratory, U.K.) and was kindly provided by Professor E. Barreto-Bergter (Instituto de Microbiologia, UFRJ, Brazil). Sterile hyphae were maintained in solid YPD [1% (w/v) yeast extract, 2% (w/v) peptone and 2% (w/v) glucose] medium and transferred in an arbitrary dilution to BHI-FCS medium containing a serial dilution of aureobasidin A or methanol.

S. cerevisiae (strain FY833) (*MAT α* , *ura3-52*, *his3 Δ 200*, *leu2 Δ 1*, *lys2 Δ 202*, *trp1 Δ 63*, *GAL2⁺*) was provided by Dr C. Masuda (Instituto de Bioquímica Médica, UFRJ, Brazil) and maintained in solid YPD medium at 28 and 4 °C. Cells were grown in liquid YPD medium at 28 °C for 48 h, collected by centrifugation (7000 g, 15 min, 4 °C), washed with cold PBS (150 mM NaCl, 10 mM NaH₂PO₄ · H₂O and 10 mM Na₂HPO₄ · 7H₂O, pH 7.4) and used for preparing the microsomal fraction.

Treatment of *C. neoformans*, *A. fumigatus* and *T. cruzi* epimastigotes with aureobasidin A or rustmicin *in vitro*

Rustmicin or aureobasidin A were kept as 10 mg · ml⁻¹ stock solutions in methanol and diluted in BHI-FCS medium just before use. Drug-free control medium always contained comparable final concentrations of methanol. Yeast forms (1 × 10⁶ ml⁻¹) of *C. neoformans* (WT and Cap67), hyphae (arbitrary dilution)

of *A. fumigatus* and epimastigotes of *T. cruzi* ($1 \times 10^6 \text{ ml}^{-1}$) were incubated in BHI-FCS medium (final volume of $200 \mu\text{l}$) containing increasing concentrations of drugs or an equivalent amount of only methanol in 96-multiwell flat-bottom plates (Corning, Corning, NY, U.S.A.) as described before [42]. After maintaining for 48 h at 37°C (*C. neoformans*) or for 72 h at 28°C (*A. fumigatus* and *T. cruzi*), the growth of yeasts or hyphae was estimated by measuring the absorbance at 560 nm (ELISA plate reader; Bio-Rad Laboratories, Hemel Hempstead, Herts., U.K.) after homogenizing each culture. The number of epimastigotes $\cdot \text{ml}^{-1}$ under different conditions was determined by direct counting using a Neubauer chamber. The IC_{50} values were determined by linear regression analysis [42].

M ϕ (murine peritoneal macrophage) infection, and rustmicin, aureobasidin A and verapamil treatments

Exudate cells removed from the peritoneal cavity of Balb/c mice were cultured in complete RPMI 1640 medium containing 2 mM L-glutamine, 1 mM sodium pyruvate, $10 \mu\text{g} \cdot \text{ml}^{-1}$ gentamicin, Eagle's-minimum-essential-medium non-essential amino acids, 10 mM HEPES, $50 \mu\text{M}$ 2-mercaptoethanol and 5% FCS at the concentration of $3 \times 10^5 \text{ cells} \cdot \text{ml}^{-1}$ on 24-well plates (Corning). M ϕ were infected with 1.0×10^6 TCT forms $\cdot \text{well}^{-1}$ in the ratio of ten parasites $\cdot \text{M}\phi^{-1}$. After 1 h, the non-internalized parasites were removed and infected M ϕ were washed three times with complete RPMI 1640 medium (1 ml each) and cultured in 1 ml of complete RPMI 1640 medium alone or a medium containing different amounts of methanol, rustmicin or aureobasidin A at 37°C under 5% CO_2 for up to 10 days. Extracellular motile trypomastigotes in the supernatants were counted after 5–10 days of infection.

To assess the number of intracellular amastigotes, M ϕ were plated on to 13-mm² coverslips (Thomas Scientific, Swedesboro, NJ, U.S.A.) inside 24-well plates, infected and treated as described above. After 3 days, the monolayers of infected M ϕ (untreated or treated with different concentrations of rustmicin, aureobasidin A, verapamil or only methanol) were washed with PBS at 37°C , fixed in methanol and Giemsa-stained. The number of amastigotes was determined by counting at least 400 M ϕ in duplicate cultures and the results were expressed as a percentage of the infected M ϕ ; the average number of amastigotes per infected M ϕ and the infection index were obtained by multiplying the percentage of infected M ϕ by the number of amastigotes inside each M ϕ .

All experimental procedures were conducted according to guidelines approved by the Committee on Ethics and Regulations of Animal Use of the Instituto de Biofísica Carlos Chagas Filho (UFRJ, Brazil).

NO production and M ϕ phagocytic capacity measurements

NO levels produced by infected and non-infected primary M ϕ cultures (assayed in quadruplicate) were estimated by reducing the nitrate accumulation for 48 h to nitric acid (over the linear range 1–80 μM) exactly as described by Saraiva et al. [43]. The phagocytic capacity of non-infected M ϕ was evaluated after 3 days of incubation in a medium containing or not verapamil, aureobasidin A or both. M ϕ were incubated with zymosan particles for 1 h (ratio of 10 particles $\cdot \text{M}\phi^{-1}$), washed, fixed, stained with Giemsa, and percentage of M ϕ -containing particles and the number of particles $\cdot \text{M}\phi^{-1}$ were determined by direct counting and used for calculating each Phagocytic Index.

Isolation of membranes

Microsomal membranes from rat liver were obtained exactly as described by Kawano et al. [44]. Protein determination, performed by the method of Lowry et al. [45], indicated that each preparation contained approx. 30–40 mg of protein $\cdot \text{ml}^{-1}$.

Microsomal membranes of *S. cerevisiae* were prepared as described by Fischl et al. [46]. Briefly, yeast cells grown in liquid YPD were collected by centrifugation (1500 g, 10 min) and washed (twice) with cold PBS. The precipitate (approx. 10 g of wet weight in each preparation) was suspended in STE buffer (25 mM Tris/HCl, pH 7.4, 250 mM sucrose and 1 mM EDTA), containing 10 mM 2-mercaptoethanol and 0.1 mM PMSF. Cell walls were disrupted with glass beads (0.15–0.21 mm; Sigma), using a Braun homogenizer (Braun, Melsungen, Germany) after 10 cycles of 1 min each with a 1 min rest on ice between each cycle. Glass beads, unbroken cells and cell-wall debris were removed by centrifugation (1500 g, 10 min) and microsomal membranes were isolated from the cellular debris after differential centrifugations at 4°C . A large granular fraction was initially removed by centrifugation at 27000 g for 10 min, and the supernatant was centrifuged at 105000 g for 90 min to obtain the small granular fraction. The pellet enriched in microsomal membranes was suspended in 4 ml of 50 mM Tris/HCl (pH 7.4) containing 5 mM 2-mercaptoethanol, 1 mM PMSF and 10% (w/v) glycerol. Aliquots of $200 \mu\text{l}$ (30–40 mg of protein $\cdot \text{ml}^{-1}$) were prepared and kept frozen at -80°C until use.

Microsomal fractions were obtained from *T. cruzi* epimastigotes as described by Previato et al. [47]. Briefly, epimastigotes grown in BHI-FCS medium (2×10^{11}) were collected by centrifugation (1500 g, 10 min) and washed (twice) with cold PBS. The pellet obtained from each culture preparation (approx. 6–7 g wet weight) was suspended in STE buffer containing 10 mM 2-mercaptoethanol and 0.1 mM PMSF. Homogenates were obtained by grinding the washed parasite pellets with liquid nitrogen. After dilution with 10–20 ml of STE containing 10 mM 2-mercaptoethanol and 0.1 mM PMSF, a post-nuclear fraction devoid of unbroken cells, nuclei and debris was prepared by centrifugation (1500 g, 10 min). The post-nuclear fraction was centrifuged at 5000 g for 10 min to remove large granules (mostly composed of mitochondria) and the supernatant was further centrifuged at 27000 g for 10 min. The supernatant was then centrifuged at 105000 g for 1 h and the resulting pellet was suspended in 50 mM Tris/HCl (pH 7.4) containing 5 mM 2-mercaptoethanol, 1 mM PMSF and 10% glycerol (20–30 mg of protein $\cdot \text{ml}^{-1}$), and aliquots of $100 \mu\text{l}$ were frozen at -80°C until use.

Total post-nuclear membrane fractions of the TCT forms were obtained from parasites collected from the supernatants of infected LLCMK₂ cell cultures. After collecting the parasites by centrifugation (1500 g, 10 min) and washing (twice) with cold PBS, the pellets were processed as above, and the microsomal fraction contained approx. 3–7 mg of protein $\cdot \text{ml}^{-1}$.

To obtain amastigotes, infected LLCMK₂ cells detached from culture flasks by trypsin were washed (four times) with cold PBS containing $1 \mu\text{g} \cdot \text{ml}^{-1}$ soya-bean trypsin inhibitor and disrupted with a tissue homogenizer pestle. The enriched amastigote fractions recovered after five centrifugations (1500 g, 10 min each) were used for the preparation of microsomal membranes (1–2 mg $\cdot \text{ml}^{-1}$ of protein) as above. The same procedure was repeated with non-infected LLCMK₂ cells as a control.

Assay for the synthesis of fluorescently labelled phosphosphingolipids

For the assays, 1 mM each of PC, PE or PI (from a 10 mM stock solution of chloroform/methanol, 1:1, v/v) was initially dried into each test tube under N_2 before the addition of $40 \mu\text{l}$ of 250 mM Tris/HCl buffer (pH 7.4) containing 25 mM EDTA and either $15 \text{ mg} \cdot \text{ml}^{-1}$ fatty-acid-free BSA or 0.25% TX-100. After sonication for 2 min in a water bath (Model T7; Thorthon-Inpec Eletrônica, Vinhedo, Sao Paulo, Brazil), 50–500 μg of microsomal protein was added and reaction started with $100 \mu\text{M}$

C₆-NBD-cer (from a 2 mM stock solution in DMSO) in a final volume of 100 μ l. Assays without phospholipids were used to correct for endogenous activity. Incubations were performed at 28 °C or 37 °C for 30 min and each reaction was terminated by the addition of 0.5 ml of 0.1 M HCl in methanol. Lipid extraction was performed with the addition of 1 ml of chloroform followed by 1.5 ml of 1 M MgCl₂ [41]. The system was centrifuged at 1500 g for 5 min and the organic phase collected and dried under a stream of N₂. The reaction products were separated on TLC using solvent system A (chloroform/methanol/water, 65:25:4, by vol.). The fluorescent labelled products were visualized with a PhosphorImager Storm 860 (Molecular Dynamics) and quantified using ImageQuant5.2.

IPC synthase activity assay

For the assay, 0.005–2 mM (final) of PI (from 0.01, 0.1, 1 and 10 mM stock solutions) was initially dried into each test tube under N₂ before the addition of 40 μ l of 250 mM Tris/maleate buffer (pH range from 3.9 to 8.1) containing or not containing 25 mM of different bivalent cations, EDTA, EGTA, DTT, NaF and 0.25 % TX-100 (w/v). When indicated, 15 mg · ml⁻¹ fatty-acid-free BSA or 25 mM CHAPS was used in replacement of TX-100. After sonication for 2 min in a water bath, 1–100 μ g of microsomal protein was added and reaction started with 1–200 μ M C₆-NBD-cer (from a 2 mM stock solution in DMSO) in a final volume of 100 μ l. Assays without PI were used to correct for endogenous activity. When present, rustmicin, aureobasidin A and/or verapamil were dried under N₂ after the PI (see above), and preincubated with microsomal membranes for 15 min at 28 °C at a final concentration of 1, 8 or 80 μ g · ml⁻¹ before the addition of C₆-NBD-cer. Incubations were performed at 4, 20, 28 or 37 °C for various times and each reaction was terminated by the addition of 0.5 ml of 0.1 M HCl in methanol. Lipid extraction was performed as above and the reaction products were separated on TLC using solvent system A. The material with relative migrations (*R_F*) of approx. 0.15 and 0.9, corresponding to IP-C₆-NBD-cer (inositol phosphoryl-C₆-NBD-cer) and unchanged C₆-NBD-cer respectively were visualized under an UV lamp and the image was digitalized with an Eagle Eye™ System (Stratagene, La Jolla, CA, U.S.A.) or with a PhosphorImager Storm 860 (Molecular Dynamics) and quantified using ImageQuant5.2. Alternatively, the products were quantified after scraping the plates, eluting the silica twice with 200 μ l of water/acetonitrile (1:1, v/v) under sonication in a water bath for 5 min followed by centrifugation at 12 000 g for 5 min. The IP-C₆-NBD-cer products recovered into each supernatant was fractionated in a Supelcosil™ LC-18 reversed-phase column (Supelco, Bellefonte, PA, U.S.A.) coupled with a Shimadzu LC-10AD HPLC system using an acetonitrile/water gradient as described by Zhong et al. [48] and were quantified by integrating the peak areas after detection with a RF10A-XL Shimadzu fluorescence detector. Using these conditions, it was defined that 6.2 × 10⁴ fluorescence units were equivalent to approx. 1 nmol, and the detection was linear between 0.01 and 40 nmol. Kinetic evaluation of substrates was performed by non-linear regression analysis using the software program Prism 3.0 (GraphPad Software). Purified IP-C₆-NBD-cer products from *S. cerevisiae* and *T. cruzi* recovered from HPLC column were collected for mild alkaline hydrolysis and PI-PLC digestions.

Mild alkaline hydrolysis and PI-PLC digestion of purified IP-C₆-NBD-cer products of *T. cruzi* and *S. cerevisiae* IPC synthase activity

Aliquots containing 50 μ g (dry weight) of IP-C₆-NBD-cer were obtained after *in vitro* synthesis by *T. cruzi* and *S. cerevisiae*

microsomal membranes and were incubated in 100 μ l of 20 mM Tris/acetate (pH 7.5)/0.1 % TX-100 for 3 h at 37 °C in the presence or absence of 0.2 unit of PI-PLC from *B. thuringiensis*. The products were recovered by 3-fold extractions with 2 vol. of butan-1-ol saturated with water and dried under a stream of N₂ [10]. Alternatively, purified IP-C₆-NBD-cer products were incubated with 20 μ l of 50 mM NaOH in 90 % (v/v) aqueous methanol or 50 mM NaCl in 90 % (v/v) aqueous methanol for 40 min at 37 °C. The treatment was terminated with 80 μ l of 20 % (v/v) acetic acid [11] followed by product extractions in butan-1-ol saturated with water as above. The products extracted were analysed by TLC using solvent system A and the same detection conditions as those used for products of the IPC synthase enzymatic assay.

RESULTS

Effects of rustmicin and aureobasidin A on fungi and different life-stage forms of *T. cruzi*

The 14-membered macrolide rustmicin (Galbonolide A) [35] and the cyclic depsipeptide aureobasidin A [49], although chemically unrelated, are potent fungicidal inhibitors of fungal IPC synthase activity and good substrates for human and yeast multi-drug efflux pumps [35,50,51]. To investigate the importance of IPC synthesis for the viability of *T. cruzi*, we evaluated the effects of these compounds on epimastigote proliferation, release of trypomastigotes from infected murine macrophages and intracellular proliferation of amastigotes, using *C. neoformans* and *A. fumigatus* as the control (Figure 1).

As expected, rustmicin (Figure 1A) and aureobasidin A (Figure 1B) inhibited the growth of the human pathogenic fungi *C. neoformans* and *A. fumigatus* with IC₅₀ comparable with literature values [33,35,52]. The results also confirmed reports of a higher resistance of *A. fumigatus* to aureobasidin A when compared with *C. neoformans* (Figure 1B). In addition, the acapsular Cap67 mutant of *C. neoformans* [40] that expresses more glycoinositolphosphorylceramides when compared with the WT [41] was 50 times more sensitive to aureobasidin A (Figure 1B), reinforcing the importance of IPC synthesis or IPC-containing molecules for fungal viability. However, neither compound affected epimastigote proliferation in axenic culture (Figures 1A and 1B).

To investigate the effects of rustmicin and aureobasidin A on infective forms of *T. cruzi*, murine peritoneal macrophages were infected with TCTs and treated with 25 μ g · ml⁻¹ of each compound (Figure 1C). After 5, 7 and 10 days of incubation, the number of trypomastigotes in the supernatant was determined. Only aureobasidin A reduced the number of released parasites when compared with control or rustmicin-treated cells (Figure 1C). Intermediate concentrations of aureobasidin A caused a dose-dependent decrease in the number of released trypomastigotes (Figure 1D), although time-dependent release also occurred in the absence of aureobasidin A (Figure 1D). These results suggested that aureobasidin A causes a dose-dependent delay in the following: differentiation of trypomastigotes to amastigotes, after entrance into the macrophage; rate of amastigote cell division; differentiation of amastigotes into trypomastigotes; or some combination of these proposed mechanisms.

To distinguish these possibilities, we examined the influence of increasing the concentration of aureobasidin A on the percentage of infected macrophages and on the number of amastigotes · macrophage⁻¹, and then calculated the infection indices (Figure 1E). Aureobasidin A treatment resulted in a small dose-dependent decrease in the percentage of infected macrophages and

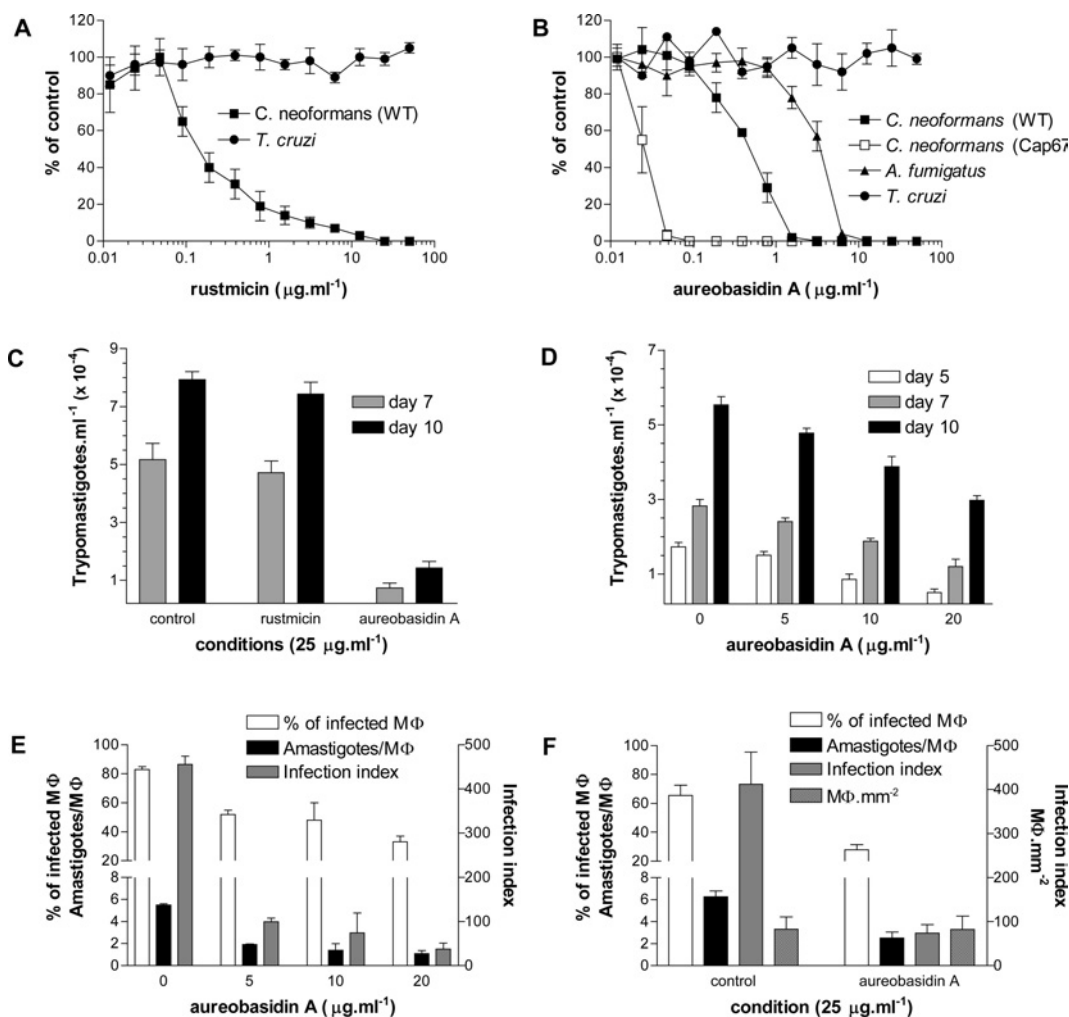


Figure 1 Effects of rustmicin and aureobasidin A on the proliferation of *C. neoformans*, *A. fumigatus* and *T. cruzi*

(A) Inhibition of growth by rustmicin was estimated in *C. neoformans* (WT) and epimastigotes of *T. cruzi* and results are expressed as a percentage of the control. (B) Same as in (A) but using aureobasidin A and *C. neoformans* (WT and Cap67), *A. fumigatus* and epimastigotes. (C) Release of trypomastigotes from infected Mφ untreated or treated with $25 \mu\text{g} \cdot \text{ml}^{-1}$ of rustmicin and aureobasidin A after 7 and 10 days of infection. (D) Same as in (C) but using increasing concentrations (0, 5, 10 and $20 \mu\text{g} \cdot \text{ml}^{-1}$) of aureobasidin A. Extracellular motile trypomastigotes in the culture supernatants were determined after 5, 7 and 10 days of infection. (E) Percentage of infected Mφ, the average number of amastigotes per infected Mφ and the infection index after 3 days of incubation in the presence of 0, 5, 10 and $20 \mu\text{g} \cdot \text{ml}^{-1}$ aureobasidin A. (F) The same as in (E) but comparing the effects of $25 \mu\text{g} \cdot \text{ml}^{-1}$ aureobasidin A with untreated control and including data about the number of Mφ $\cdot \text{mm}^{-2}$. Results shown are means \pm S.D. of three sets of independent experiments.

in the number of amastigotes \cdot macrophage $^{-1}$ giving a 5–6-fold decrease in the infection index (Figure 1E). However, no intermediary forms were present in the macrophages. At $25 \mu\text{g} \cdot \text{ml}^{-1}$ (Figure 1F), the percentage of infected macrophages decreased from 70 to 30% and the average number of amastigotes from 6 to 3. The number of macrophages $\cdot \text{mm}^{-2}$ did not change compared with untreated control cultures, eliminating aureobasidin A-mediated effects on attachment to the coverslips or viability of the macrophages (Figure 1F).

These results suggested that aureobasidin A interferes with the differentiation of trypomastigotes into amastigotes after cell entry, leading to a decrease in the percentage of infected macrophages. The persistence of intracellular amastigotes in all treated cultures suggests that aureobasidin A may also interfere with the amastigotes' cell cycle, preventing their proliferation and re-differentiation into trypomastigotes. However, on the basis of the present results, we cannot exclude the possibility that the effect of aureobasidin A on amastigote proliferation is not due to an effect on macrophage function.

Identification of IPC synthase activity in the microsomes of *T. cruzi*

Since, in yeast, the target of aureobasidin A is IPC synthase [31], we attempted to detect this activity in *T. cruzi*. First, microsomal membranes were prepared from epimastigotes and, using rat liver and *S. cerevisiae* microsomal preparations as controls, phosphosphingolipid synthesis was monitored using PC, PE and PI as donor substrates and fluorescent C₆-NBD-cer as the acceptor substrate (Figure 2). As expected, rat liver microsomes were capable of synthesizing phosphosphingolipids especially when incubated in the presence of fluorescent C₆-NBD-cer and PC, probably forming sphingomyelin-C₆-NBD-cer (Figure 2A). Only small amounts of phosphosphingolipids were detected over background labelling when PE or PI was used as the substrate (Figure 2B). Similar results were observed for *T. cruzi* microsomal membranes, except that the addition of PI gave rise to a strong fluorescent band (Figures 2A and 2B). The appearance of a fluorescent band only after the addition of PI when using *S. cerevisiae* microsomal membranes confirmed that the exogenously added substrates PC, PE

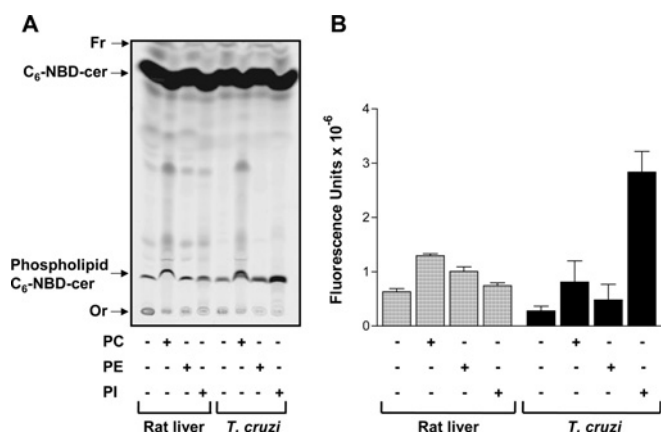


Figure 2 Fluorescent phosphosphingolipids synthesized by rat liver and epimastigote microsomal membranes

(A) Membranes ($100 \mu\text{g} \cdot \text{ml}^{-1}$) were incubated in $100 \mu\text{l}$ of 100 mM Tris/HCl (pH 7.4) containing 0.1 mM $\text{C}_6\text{-NBD-cer}$, $6 \text{ mg} \cdot \text{ml}^{-1}$ fatty-acid-free BSA (rat liver) or 0.1% TX-100 (*T. cruzi*), in the absence (–) or presence (+) of 1 mM PC, PE or PI. After 30 min of incubation at 37°C (rat liver) or 28°C (*T. cruzi*), lipids were extracted, separated by TLC and visualized using a PhosphorImager Storm 860 (Molecular Dynamics). The relative positions of synthesized phosphosphingolipids labelled with $\text{C}_6\text{-NBD-cer}$ and unchanged $\text{C}_6\text{-NBD-cer}$ are indicated on the left, together with the origin (Or) and the front (Fr) of the chromatogram. (B) Fluorescence intensities of synthesized phosphosphingolipids containing $\text{C}_6\text{-NBD-cer}$ from three independent experiments (means \pm S.E.M.) were quantified using ImageQuant5.2.

and PI were not cross-contaminated, since yeast is known to transfer neither choline phosphate nor EtNP to ceramide, but only inositol phosphate (see Supplementary Figure 1 at <http://www.BiochemJ.org/bj/387/bj3870519add.htm>). Taken together, the results suggest that, as happens with *S. cerevisiae* but not with rat liver, *T. cruzi* microsomal membranes contain an IPC synthase activity.

In both *S. cerevisiae* and *T. cruzi*, the detected IPC synthase activity required the presence of non-heat-inactivated microsomes and was stimulated by the addition of exogenous PI (Figure 3). The activity observed in the absence of exogenous PI suggests that considerable amounts of PI are present in the microsomal preparation, and this activity can vary from one preparation to another (N. Heise, unpublished work). As expected, rustmicin and aureobasidin A completely inhibited yeast IPC synthase but, surprisingly, had no effect on the *T. cruzi* enzyme, even in 1000-fold excess (Figure 3) and in combination (see Supplementary Figure 2 at <http://www.BiochemJ.org/bj/387/bj3870519add.htm>).

The relative ineffectiveness of these inhibitors against the trypanosomal enzyme suggests either that it is structurally divergent from other IPC synthases or that the reaction in *T. cruzi* is mechanistically distinct from that in yeast and plants. However, since the reactions were performed in crude microsomal membranes, we cannot disregard at this point the possibility that the lack of inhibition of IPC synthase by either rustmicin or aureobasidin A in *T. cruzi* could be due to factors other than the structural difference between the *T. cruzi* enzyme and that from *S. cerevisiae*. To address this hypothesis, we have prepared an experiment where the IPC synthase reaction was performed mixing both microsomal membranes together and incubating the mixture in the absence or presence of rustmicin or aureobasidin A (Figure 4). The mixture of membranes was prepared in such a way that each source contributed about half of the total synthesized IP- $\text{C}_6\text{-NBD-cer}$, and the results clearly show that there is no factor in the *T. cruzi* membranes that could interfere with the inhibition of *S. cerevisiae* IPC synthase by rustmicin or aureobasidin A (Figures 4A and 4B).

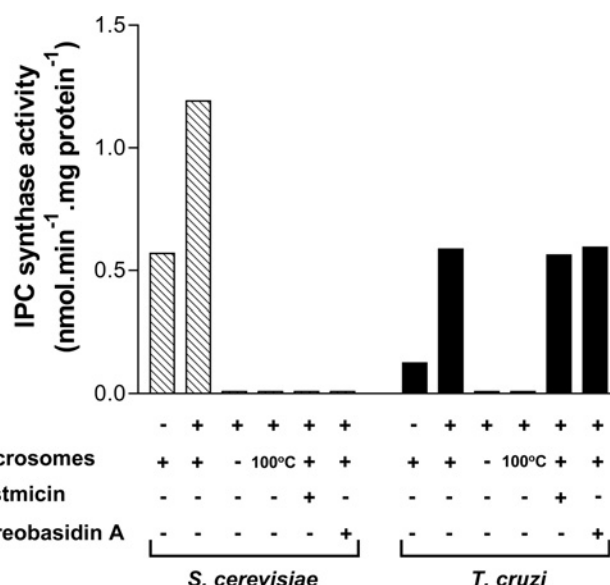


Figure 3 IPC synthase activity in *S. cerevisiae* and *T. cruzi* microsomal membranes

Membranes prepared from *S. cerevisiae* and epimastigotes of *T. cruzi* were incubated in $100 \mu\text{l}$ of 100 mM Tris/maleate (pH 6.0), 1 mM PI, 0.1 mM $\text{C}_6\text{-NBD-cer}$ and $6 \text{ mg} \cdot \text{ml}^{-1}$ fatty-acid-free BSA. Control reactions without PI or microsomes or using heat-inactivated microsomes (100°C) were also included as indicated. When present, rustmicin or aureobasidin A was preincubated with microsomal membranes for 15 min at a final concentration of $8 \mu\text{g} \cdot \text{ml}^{-1}$ before the addition of $\text{C}_6\text{-NBD-cer}$. Lipid extractions and the quantification of IP- $\text{C}_6\text{-NBD-cer}$ were performed as described in the Experimental section.

Characterization of the reaction product

The IP- $\text{C}_6\text{-NBD-cer}$ produced by *S. cerevisiae* or epimastigotes membranes was purified as described in the Experimental section, and approx. $50 \mu\text{g}$ (dry weight) of each was treated with PI-PLC or mild alkali (Figure 5) and analysed by TLC. As expected, untreated purified products co-migrated with authentic yeast IP- $\text{C}_6\text{-NBD-cer}$ and were stable to mild alkaline hydrolysis in 50 mM methanolic NaOH for 40 min at 37°C . PI-PLC digestion, however, resulted in its degradation and the concomitant appearance on the TLC of the corresponding $\text{C}_6\text{-NBD-cer}$ (Figure 5), thus confirming that the reaction product was IPC.

Characterization of enzyme activity

To characterize the IPC synthase activity from *T. cruzi* epimastigotes, several kinetic parameters were determined (Figure 6). Product formation was linear for at least 15 min (Figure 6A) and was proportional to the amount of microsomal membrane protein added (Figure 6B). IP- $\text{C}_6\text{-NBD-cer}$ formation was dependent on the presence of $\text{C}_6\text{-NBD-cer}$ (Figure 6C) and PI (Figure 6D). Maximum enzyme activity was observed at pH 6.0, with half-maximum activity observed at pH 5.0 and 7.0 (Figure 6E). The optimum pH was, respectively, 1.0 and 1.8 pH units lower than that reported for the enzymes (results not shown) of yeast [46] and wax bean [53]. Surprisingly, epimastigote IPC synthase activity was maximal at approx. 37°C (Figure 6F), with very little activity at 4°C or above 40°C (results not shown).

The effects of bivalent cations, chelators, BSA and detergents were also assessed (Table 1). Activity was slightly decreased in the presence of 10 mM MgCl_2 , CaCl_2 and MnCl_2 , but was strongly impaired by similar concentrations of NiCl_2 , CoCl_2 and CuCl_2 . Although some previous studies of *S. cerevisiae* IPC synthase have included Mg^{2+} and Mn^{2+} ions in the assay system [27,46,54],

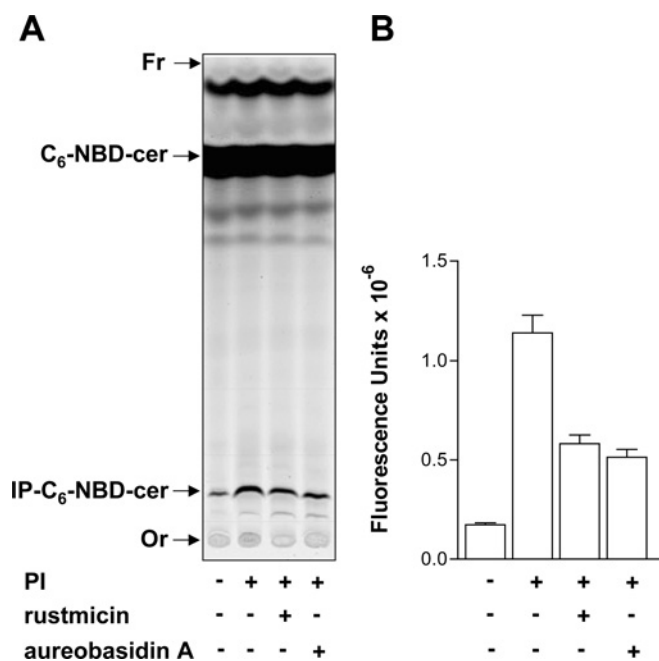


Figure 4 Effects of rustmucin and aureobasidin A on the IPC synthase activity of mixed microsomal membranes from *S. cerevisiae* and epimastigotes

(A) Microsomal membranes from both *S. cerevisiae* ($50 \mu\text{g} \cdot \text{ml}^{-1}$) and epimastigotes ($100 \mu\text{g} \cdot \text{ml}^{-1}$) were incubated together in $100 \mu\text{l}$ of Tris/HCl (pH 7.4), $6 \text{ mg} \cdot \text{ml}^{-1}$ fatty-acid-free BSA and 0.1 mM $\text{C}_6\text{-NBD-cer}$ in the absence (–) or presence (+) of PI, rustmucin or aureobasidin A as indicated. After 30 min of reaction at 28°C , lipids were extracted, separated by TLC and visualized using a PhosphorImager Storm 860. The relative positions of synthesized $\text{IP-C}_6\text{-NBD-cer}$ and unchanged $\text{C}_6\text{-NBD-cer}$ are indicated on the left, together with the origin (Or) and the front (Fr) of the chromatogram. (B) Fluorescence intensities of $\text{IP-C}_6\text{-NBD-cer}$ synthesized from two independent experiments (means \pm S.E.M.) were quantified using ImageQuant5.2.

others have omitted them [31,48]. Assays of the yeast enzyme activity typically included detergent [27,31,46,48,54]. As shown in Table 1, although CHAPS had no effect, fatty-acid-free BSA compromised the *T. cruzi* IPC synthase activity. Unlike the yeast [48] and plant [53] IPC synthases, which are 75% inhibited by 0.1% TX-100, the *T. cruzi* enzyme was stimulated in the presence of 0.1% TX-100 and the activity was even higher when assayed in the presence of 10 mM EDTA, EGTA or DTT (Table 1).

Using optimized assay conditions for the epimastigote IPC synthase, K_m (app) values of 592 ± 191 and $74 \pm 11 \mu\text{M}$ were obtained for PI and $\text{C}_6\text{-NBD-cer}$ respectively. K_m (app) = $500 \mu\text{M}$ was reported for PI with the IPC synthase of yeast [48] and K_m (app) = $200 \mu\text{M}$ for the enzyme from wax bean [53]. In contrast, the K_m (app) of the yeast enzyme for $\text{C}_6\text{-NBD-cer}$ was determined to be $9.8 \mu\text{M}$ [48]. These calculations allow for the contribution of endogenous PI or ceramide and so may be underestimates; however, using optimized conditions, the approximate specific activity of microsomal epimastigote IPC synthase was $12.5 \pm 1.5 \text{ nmol} \cdot \text{min}^{-1} \cdot (\text{mg of protein})^{-1}$, a value approx. 20 times higher than that observed for the enzyme of yeast (Figure 3 and [48]) and wax bean [53].

IPC synthase activity in all life-cycle stages of *T. cruzi*

Since IPC synthase from *T. cruzi* epimastigotes was not inhibited by rustmucin and aureobasidin A, but the latter interfered with the differentiation or cell cycle of intracellular forms of *T. cruzi* (Figures 1C–1F), we also tested aureobasidin A on the IPC syn-

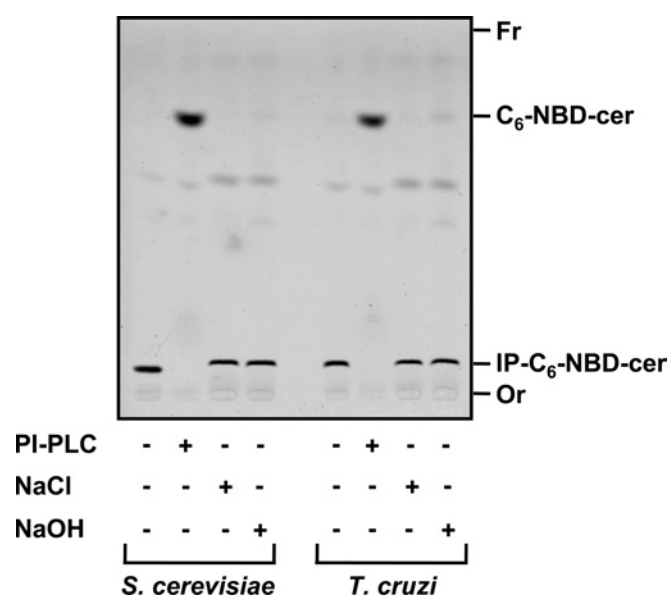


Figure 5 Characterization of the $\text{IP-C}_6\text{-NBD-cer}$ products synthesized by *S. cerevisiae* and *T. cruzi* microsomal membranes

Equivalent amounts of purified $\text{IP-C}_6\text{-NBD-cer}$ synthesized by microsomal membranes derived from *S. cerevisiae* and *T. cruzi* epimastigotes were incubated with buffer only or with 0.2 unit of PI-PLC from *B. thuringiensis* (PI-PLC), 50 mM NaCl in 90% aqueous methanol or 50 mM NaOH in 90% aqueous methanol as described in the Experimental section and the products were analysed by TLC using solvent system A. The materials with relative migrations $R_f \sim 0.15$ and ~ 0.9 , corresponding respectively to intact $\text{IP-C}_6\text{-NBD-cer}$ and $\text{C}_6\text{-NBD-cer}$ released from the former after PI-PLC digestion, were digitalized from the TLC with a PhosphorImager Storm 860. The origin (Or) and the front (Fr) of the chromatogram are also indicated.

thase activity of different membrane preparations from TCTs and amastigotes, and the results are shown in Figure 7. As shown before, yeast IPC synthase was inhibited (yeast; Figures 7A and 7B), but the enzyme from *T. cruzi* epimastigotes (EPI; Figures 7A and 7B), TCTs (Figures 7A and 7B) and amastigotes (AMA; Figures 7A and 7B) was not. The same results were obtained using 1 or $8 \mu\text{g} \cdot \text{ml}^{-1}$ rustmucin and both aureobasidin A and rustmucin in combination, in assays at either pH 5.5 or 7.0 (results not shown). A maximum of 30% inhibition could be observed only when $80 \mu\text{g} \cdot \text{ml}^{-1}$ aureobasidin A was used (Figure 7B, AMA and TCTs). These results suggest that the fungicidal agent aureobasidin A is toxic against infective stage forms of *T. cruzi*, but, in contrast with fungi, toxicity is not mediated by inhibition of IPC synthase.

Further insight into the mode of action of aureobasidin A on parasite growth

Although considered non-toxic to mammals [32,33], it has been shown previously that aureobasidin A is a good substrate for human and yeast multidrug ABC transporters [50,51]. To test if this possible interaction could be related to the inhibitory effects of aureobasidin A on the intracellular parasites, we have compared the effects of the mammalian multidrug-resistance modulator verapamil on parasite susceptibility to aureobasidin A (Figure 8A). Treatment of verapamil alone resulted in a small decrease in the percentage of infected $\text{M}\phi$ and in the number of amastigotes per $\text{M}\phi$, giving only a 2–3-fold decrease in the infection index. These effects were comparable with that of aureobasidin A, but they were not enhanced significantly when cells were incubated with both drugs together. As observed before (Figure 1F), the number of $\text{M}\phi \cdot \text{mm}^{-2}$ did not change when compared with untreated control cultures (Figure 8A).

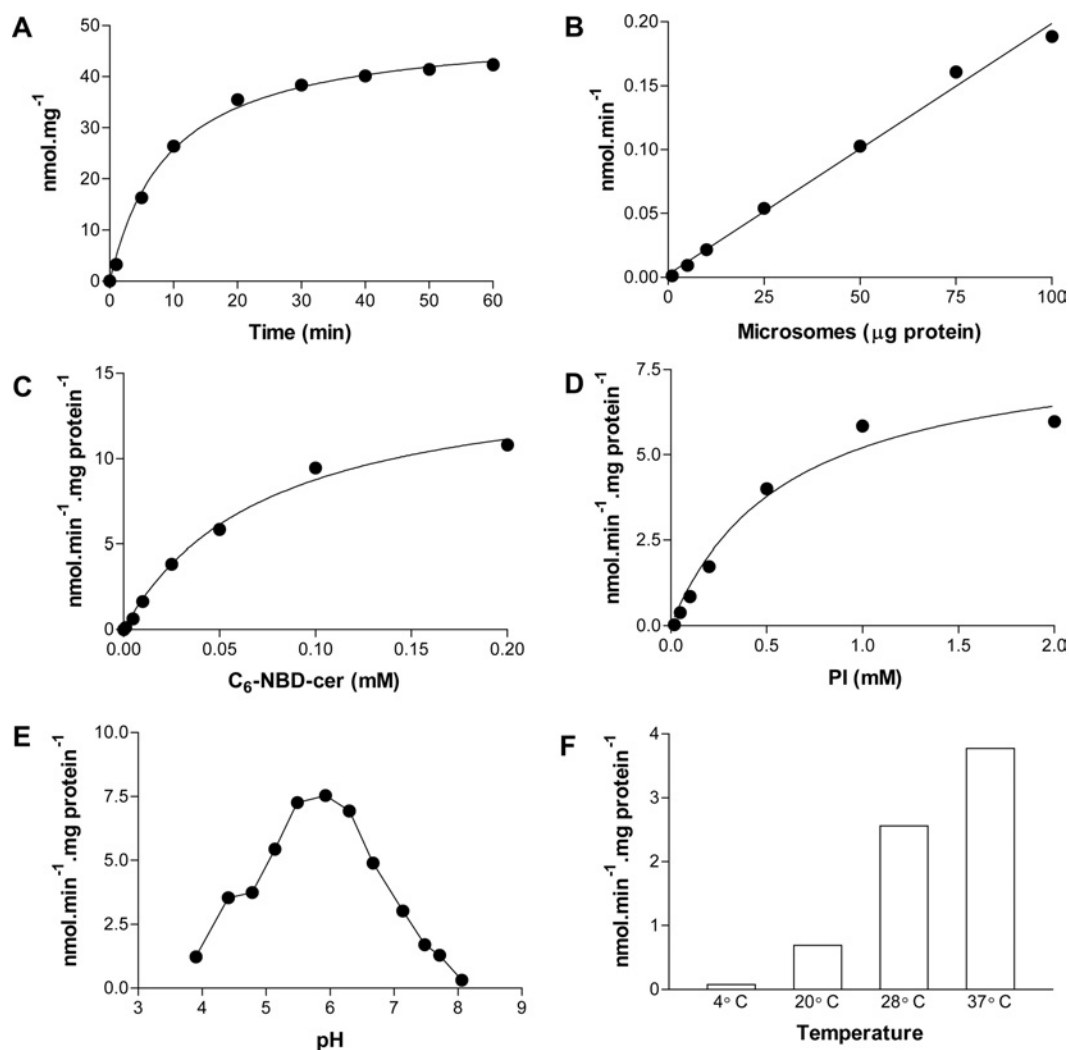


Figure 6 Characterization of the *T. cruzi* IPC synthase

(A) Assays in 100 μ l containing 100 mM Tris/HCl (pH 7.4), 10 mM MgCl₂, 6 mg \cdot ml⁻¹ BSA, 1 mM PI, 100 μ M C₆-NBD-cer and 100 μ g \cdot ml⁻¹ microsomal membranes were performed at 28 °C for 0, 2, 5, 10, 20, 30, 40, 50 and 60 min. Lipid extractions and the quantification of IP-C₆-NBD-cer were performed as described in the Experimental section. (B) Measurements were performed as in (A) but using 0, 5, 10, 25, 50, 75 and 100 μ g \cdot ml⁻¹ microsomal membranes and incubation for 30 min. (C) Assays were performed in 100 μ l containing 100 mM Tris/maleate (pH 6.0), 10 mM EDTA, 0.1 % TX-100, 1 mM PI, 100 μ g \cdot ml⁻¹ microsomal membranes and 0, 3.125, 6.25, 12.5, 25, 50, 100 and 200 μ M C₆-NBD-cer. After maintaining for 15 min at 28 °C, the synthesized IP-C₆-NBD-cer was extracted and quantified as above. (D) The same as in (C) but using 200 μ M C₆-NBD-cer and 0, 0.06, 0.125, 0.25, 0.5, 1 and 2 mM PI in the assay mix. (E) The pH dependence of IPC synthase was measured after the incubation of microsomal membranes (100 μ g \cdot ml⁻¹) in 100 μ l containing 0.1 % TX-100, 1 mM PI, 100 μ M C₆-NBD-cer and 100 mM Tris/maleate (pH 3.9, 4.4, 4.7, 5.1, 5.5, 5.9, 6.3, 6.7, 7.1, 7.5, 7.7 and 8.1) for 30 min at 28 °C. (F) Using the same conditions as in (A), activity was measured for 30 min at 4, 20, 28 and 37 °C.

To test the effects of these drugs on M ϕ function, infected and non-infected M ϕ were incubated in the presence and absence of LPS + IFN- γ and the presence or absence of verapamil, aureobasidin A or both. After 2 days of incubation, the amounts of NO in the supernatants of each culture were determined and the results are presented in Figure 8(B). As expected, whereas the classical M ϕ activator LPS + IFN- γ induced the secretion of large amounts of NO, infection of M ϕ with TCTs did not [43]. The addition of verapamil, aureobasidin A or both to non-infected M ϕ cultures did not cause any change in the basal levels of NO (Figure 8B). However, when infected or non-infected M ϕ were incubated with LPS + IFN- γ and the drugs, a considerable decrease in NO production was observed, especially when aureobasidin A was used (Figure 8B). Finally, non-infected M ϕ showed a 50 % decrease in their phagocytic capacity after 3 days of treatment with aureobasidin A, but not with verapamil (see Supplementary Figure 3 at <http://www.BiochemJ.org/bj/387/>

<http://www.BiochemJ.org/bj/387/519add.htm>). Taken together, the results suggest that the inhibitory effects of aureobasidin A on intracellular *T. cruzi* proliferation may be due to an effect on M ϕ function. However, more extensive studies on these effects are underway to establish their molecular basis.

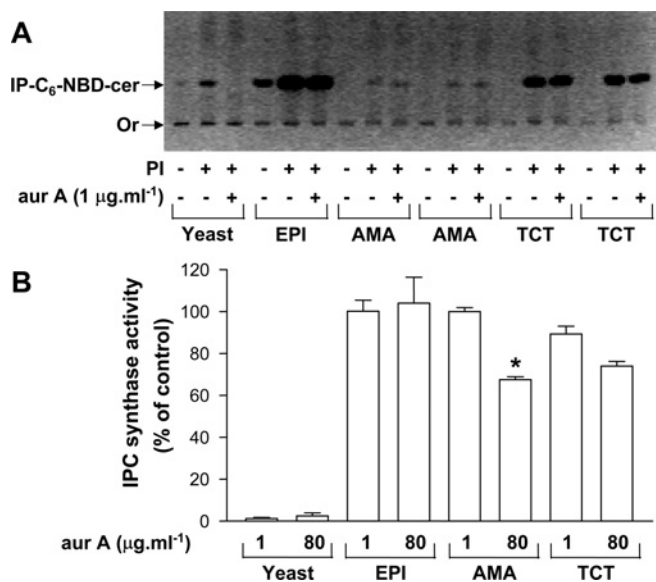
DISCUSSION

Characterization of IPC synthase activity in the protozoan parasite *T. cruzi* has been reported for the first time in this paper. The enzyme activity detected in microsomal preparations from all life-cycle stages suggests that the reaction products, including, probably, the complex glycopospholipids, are similar and common to all forms of the parasite. The properties of the enzymatic activity are consistent with the reaction scheme proposed for the IPC synthase of fungi and plants. However, the optimum pH of the *T. cruzi* enzyme (pH 6.0) differs from that

Table 1 Effects of several agents on the activity of *T. cruzi* IPC synthase in the absence or presence of TX-100

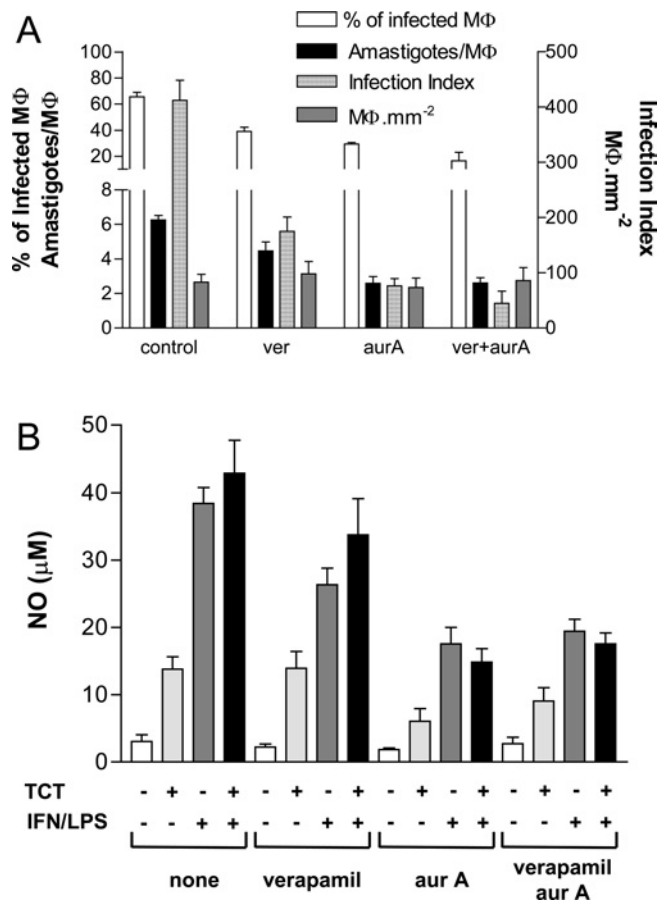
Assays were performed in a final volume of 100 μ l containing 100 mM Tris/maleate (pH 6.0), 1 mM PI, 100 μ g of microsomal protein and 0.1 mM C_6 -NBD-cer at 28 °C for 30 min. All metal ions were added as the chloride salt. n.d., not determined.

Conditions	Activity [$\text{nmol} \cdot \text{min}^{-1} \cdot (\text{mg of protein})^{-1}$]	
	Without TX-100	With 0.1 % TX-100
Without PI	0.1482	0.5190
PI	2.1092	5.0161
PI + 10 mM Mg^{2+}	1.7765	3.6726
PI + 10 mM Mn^{2+}	0.7577	1.7343
PI + 10 mM Ca^{2+}	1.4143	3.7845
PI + 10 mM Ni^{2+}	0.2124	0.1239
PI + 10 mM Co^{2+}	0.2320	0.2497
PI + 10 mM Cu^{2+}	0.0260	0.0080
PI + 6 mg $\cdot \text{ml}^{-1}$ BSA	0.5913	n.d.
PI + 10 mM CHAPS	2.0534	n.d.
PI + 10 mM EGTA	2.0671	8.0764
PI + 10 mM EDTA	2.1856	9.1979
PI + 10 mM DTT	2.6906	6.2430
PI + 10 mM NaF	1.9505	4.8157

**Figure 7** Effects of aureobasidin A (aurA) on the IPC synthase activity of microsomes obtained from *S. cerevisiae* and different life-cycle stages of *T. cruzi*

(A) Microsomal membranes prepared from *S. cerevisiae* (100 $\mu\text{g} \cdot \text{ml}^{-1}$; yeast), epimastigotes (EPI; 100 $\mu\text{g} \cdot \text{ml}^{-1}$) and two sources of tissue culture-derived amastigotes (AMA, 50 $\mu\text{g} \cdot \text{ml}^{-1}$) and TCTs (50 $\mu\text{g} \cdot \text{ml}^{-1}$) were preincubated in 100 μl of 100 mM Tris/maleate (pH 6.0), 10 mM EDTA and 0.1 % TX-100 at 28 °C for 15 min in the absence (–) or presence (+) of 1 mM PI and/or 1 $\mu\text{g} \cdot \text{ml}^{-1}$ aurA. The assay was started with the addition of 0.1 mM C_6 -NBD-cer and incubations were held at 28 °C for 30 min. Lipids were extracted and visualized under an UV lamp and the image was digitalized with an Eagle Eye™ System of the TLC selected to emphasize the origin (Or), and the relative position of IP- C_6 -NBD-cer is shown in the negative mode. (B) Inhibition of IPC synthase activity by 1 and 80 $\mu\text{g} \cdot \text{ml}^{-1}$ aurA when compared with untreated controls using different sources of microsomal membranes. Results are means \pm S.E.M. for three (yeast, EPI and TCT) or two (AMA) independent experiments performed in duplicate. The significance of the observed inhibition using 80 $\mu\text{g} \cdot \text{ml}^{-1}$ aurA (AMA) was calculated by the Student's *t* test and considered significant (**P* < 0.05).

of yeast (pH 7.0) and wax bean (pH 7.8). In addition, rustmicin and aureobasidin A, two chemically unrelated inhibitors of all hitherto described fungal and plant IPC synthases, did not inhibit

**Figure 8** Effects of verapamil, aureobasidin A (aurA) and both together on the percentage of infected M ϕ , the number of amastigotes per infected M ϕ and the release of NO by infected and non-infected M ϕ

(A) Coverslips plated with murine peritoneal M ϕ were infected with TCT forms of *T. cruzi* (in the ratio of 5 parasites $\cdot \text{M}\phi^{-1}$) for 1 h, washed and incubated with fresh medium alone (control) or a medium containing 1 $\mu\text{g} \cdot \text{ml}^{-1}$ verapamil (ver), 25 $\mu\text{g} \cdot \text{ml}^{-1}$ aurA or both (ver + aurA) as indicated. After 3 days, the coverslips were fixed and stained with Giemsa, and the percentage of infected M ϕ as well as the number of amastigotes $\cdot \text{M}\phi^{-1}$, the average number of amastigotes per infected M ϕ and the number of M ϕ $\cdot \text{mm}^{-2}$ were determined by direct counting. Results are the means \pm S.D. for three independent experiments. (B) Plated M ϕ were infected (+) or not (–) with TCT forms of *T. cruzi* for 1 h, washed and then incubated with fresh medium containing (+) or not containing (–) LPS + IFN- γ in the absence or presence of 1 $\mu\text{g} \cdot \text{ml}^{-1}$ verapamil, 25 $\mu\text{g} \cdot \text{ml}^{-1}$ aurA or both verapamil and aurA as indicated at the bottom. After 2 days of culture, aliquots of the supernatant were taken for the measurement of level of production of NO. The graph represents the mean values of duplicate measurements from two independent experiments.

the *T. cruzi* enzyme. IPC synthase assay measurements performed with mixed microsomal membranes from yeast and *T. cruzi* suggest that the lack of inhibition by either rustmicin or aureobasidin A in *T. cruzi* was not due to factors present in the parasites' extracts. Therefore the toxicity of aureobasidin A to infective forms of *T. cruzi* was probably not mediated by the inhibition of IPC synthase but, instead, by an effect on macrophage function, since, regardless of infection, treated cells presented a diminished phagocytic capacity and were unable to produce normal levels of NO when stimulated with LPS + IFN- γ . The relative inefficiency of rustmicin and aureobasidin A against the trypanosomal enzyme suggests that its sequence may be divergent from fungal IPC synthases or that the reaction catalysed by the *T. cruzi* enzyme may be mechanistically distinct.

We have previously characterized the precursors of the GPI protein anchors of *T. cruzi* [11]. Although several GPI-anchored proteins and GIPLs are linked to IPC, the GPI precursors are

synthesized neither by live parasites nor in a cell-free system contained ceramide [11]. Interestingly, ceramide is also absent from the complete GPI anchor precursors of yeast [56]. In yeast, the introduction of ceramide into GPI anchors is thought to be mediated by the same type of head group exchange that occurs in IPC synthesis (i.e. transfer of inositol phosphate from glycerolipid to a ceramide). It is possible, therefore, that lipid remodelling similar to that observed in some GPI-anchored proteins [24–26] and IPC [27] from *S. cerevisiae* occurs in *T. cruzi* [11,55]. However, it is already known that IPC synthase is not involved in yeast lipid remodelling, since the reaction is not inhibited by aureobasidin A and does not use IPC as the substrate [24–26]. Recent studies have identified phospholipases in *T. cruzi* that are active on both PI and IPC and could therefore be involved in remodelling [55,57–59]. Therefore it should be investigated in the future whether aureobasidin A has any effect on putative ceramide remodelling reactions that could be responsible for introducing ceramide into the GPI anchors of *T. cruzi*. However, there is no direct evidence yet of this phenomenon occurring in *T. cruzi*.

Previous studies have identified a gene (*AUR1*) in *S. cerevisiae* that confers resistance to aureobasidin A [60] and which is essential, since mutants lacking it are not viable [31,61]. It has been shown that the *AUR1* gene product, which is required for the synthesis of IPC, is located in the Golgi [54], but it is not clear whether the Aur1 protein is IPC synthase itself or a regulator of its activity, since IPC synthase has not been purified yet [62]. To date, homologues of the *AUR1* gene have been identified only in fungi and contain a conserved structural motif for inositol phosphoryltransferases, which is similar to a motif described for lipid phosphatases [63], but with unique characteristics [60]. The sequences of Aur1 proteins are well conserved in the putative membrane-spanning domains present in their central regions and in the amino acid composition of the three domains that compose the catalytic triad [60]. BLAST searches using conserved fungal Aur1 protein sequences did not retrieve homologous sequences from the *T. cruzi* genome, and touch-down PCRs using degenerate primers gave, so far, no amplicons when using total *T. cruzi* genomic DNA as the template (N. Heise, unpublished work).

Homologues of the *AUR1* gene of *S. cerevisiae* that confer resistance to aureobasidin A have been reported in other fungi, including *Schizosaccharomyces pombe* [64] and *Aspergillus* [65]. Although the sequences of these proteins are conserved in their central regions, their N- and C-termini are divergent [65]. Single amino acid mutations in the conserved catalytic domains may be sufficient to confer aureobasidin A resistance [31,61]. Furthermore, it is probable that the C-terminal regions of the Aur1 proteins of *S. cerevisiae* and *S. pombe* are important for the maintenance of the Aur1 activity, since IPC synthase activity is lost when the C-terminus is deleted by a frame-shift mutation [31,64]. Moreover, mutation of His-294 of *AUR1* of *S. cerevisiae*, located in a putative active site identified upstream of the most C-terminal transmembrane domain and believed to be facing the Golgi lumen, results in non-viable haploid cells [54]. Careful studies by Zhong et al. [48,52] indicate that aureobasidin A acts as a tight-binding non-competitive inhibitor with respect to C₆-NBD-cer. This suggests that aureobasidin A binds to a distinct hydrophobic site on IPC synthase that is conserved between different fungal species [48]. Taken together with our results, these observations suggest that *T. cruzi* IPC synthase has a structure different from that of fungi and plants, which may be sufficient to impair inhibition by rustmicin and aureobasidin A. Therefore purification and molecular characterization of the trypanosomal IPC synthase, leading to the discovery of effective inhibitors, will be necessary to validate the SBP as a target for chemotherapy against Chagas disease.

We thank O. A. A. Filho for technical assistance, Professor F. R. Opperdoes and Dr S. B. Levery for providing some of the reagents used in this study, Dr S. Ferreira for access to the HPLC fluorescence detector, and Dr R. Wait and Dr C. West for a critical reading of this paper. This work was supported by grants from the Conselho Nacional de Desenvolvimento Científico e Tecnológico, Fundação de Amparo à Pesquisa do Estado do Rio de Janeiro, PADCT-FAPERJ, Third World Academy of Sciences and the International Foundation for Science. J. O. P. was partially supported by a fellowship from the John Simon Guggenheim Memorial Foundation and J. M. F. and W. B. D. were recipients of Ph.D. fellowships from the Coordenadoria de Aperfeiçoamento de Ensino Superior.

REFERENCES

- Moncayo, A. (2003) Chagas disease: current epidemiological trends after the interruption of vectorial and transfusional transmission in the Southern cone countries. *Mem. Inst. Oswaldo Cruz* **98**, 577–591
- Tyler, K. M. and Engman, D. M. (2001) The life cycle of *Trypanosoma cruzi* revisited. *Int. J. Parasitol.* **31**, 472–481
- Cardoso de Almeida, M. L. and Heise, N. (1993) Proteins anchored via GPI and solubilizing phospholipases in *Trypanosoma cruzi*. *Biol. Res.* **26**, 285–312
- McConville, M. J. and Ferguson, M. A. J. (1993) The structure, biosynthesis and function of glycosylated phosphatidylinositols in the parasitic protozoa and higher eukaryotes. *Biochem. J.* **294**, 305–324
- Previato, J. O., Wait, R., Jones, C., DosReis, G. A., Todeschini, A. R., Heise, N. and Mendonça-Previato, L. (2004) Glycoinositolphospholipid (GIPL) from *Trypanosoma cruzi*: structure, biosynthesis and immunology. *Adv. Parasitol.* **56**, 1–41
- Burleigh, B. A. and Andrews, N. W. (1995) Mechanisms of *Trypanosoma cruzi* invasion of mammalian cells. *Annu. Rev. Microbiol.* **49**, 175–200
- Schenkman, S., Ferguson, M. A. J., Heise, N., Cardoso de Almeida, M. L., Mortara, R. A. and Yoshida, N. (1993) Mucin-like glycoproteins linked to the membrane by glycosylphosphatidylinositol anchor are the major acceptors of sialic acid in a reaction catalyzed by *trans*-sialidase in metacyclic forms of *Trypanosoma cruzi*. *Mol. Biochem. Parasitol.* **59**, 293–303
- Previato, J. O., Jones, C., Xavier, M. T., Wait, R., Travassos, L. R., Parodi, A. J. and Mendonça-Previato, L. (1995) Structural characterization of the major glycosylphosphatidylinositol membrane-anchored glycoprotein from epimastigote forms of *Trypanosoma cruzi* Y-strain. *J. Biol. Chem.* **270**, 7241–7250
- Serrano, A. A., Schenkman, S., Yoshida, N., Mehler, A., Richardson, J. M. and Ferguson, M. A. J. (1995) The lipid structure of the GPI-anchored mucin-like sialic acid acceptors of *Trypanosoma cruzi* changes during parasite differentiation from epimastigotes to infective metacyclic trypomastigote forms. *J. Biol. Chem.* **270**, 27244–27253
- Heise, N., Cardoso de Almeida, M. L. and Ferguson, M. A. J. (1995) Characterization of the lipid moiety of the glycosylphosphatidylinositol anchor of *Trypanosoma cruzi* 1G7-antigen. *Mol. Biochem. Parasitol.* **70**, 71–84
- Heise, N., Raper, J., Buxbaum, L. U., Peranovich, T. M. S. and Cardoso de Almeida, M. L. (1996) Identification of complete precursors for the glycosylphosphatidylinositol protein anchors of *Trypanosoma cruzi*. *J. Biol. Chem.* **271**, 16877–16887
- Ferguson, M. A. J. (2000) Glycosylphosphatidylinositol biosynthesis validated as drug target for African sleeping sickness. *Proc. Natl. Acad. Sci. U.S.A.* **97**, 10673–10675
- Raiton, J. E. and McConville, M. J. (1998) Delineation of three pathways of GPI biosynthesis in *Leishmania mexicana*: precursors from different pathways are assembled on distinct pools of PI and undergo fatty acid remodelling. *J. Biol. Chem.* **273**, 4245–4257
- Güther, M. L. S., Cardoso de Almeida, M. L., Yoshida, N. and Ferguson, M. A. J. (1992) Structural studies on the GPI membrane anchor of *Trypanosoma cruzi* 1G7-antigen. *J. Biol. Chem.* **267**, 6820–6828
- Almeida, I. C., Ferguson, M. A. J., Schenkman, S. and Travassos, L. R. (1994) Lytic anti- α -galactosyl antibodies from patients with chronic Chagas disease recognize novel O-linked oligosaccharides on mucin-like glycosylphosphatidylinositol anchored glycoproteins of *Trypanosoma cruzi*. *Biochem. J.* **304**, 793–802
- Almeida, I. C., Camargo, M. M., Procópio, D. O., Silva, L. S., Mehler, A., Travassos, L. R., Gazzinelli, R. T. and Ferguson, M. A. J. (2000) Highly purified glycosylphosphatidylinositols from *Trypanosoma cruzi* are potent proinflammatory agents. *EMBO J.* **19**, 1476–1485
- De Lederkremer, R. M., Lima, C. E., Ramirez, M. I., Goçálvos, M. F. and Colli, W. (1993) Hexadecylpalmitoylglycerol or ceramide is linked to similar glycoposphoinositol anchor-like structures in *Trypanosoma cruzi*. *Eur. J. Biochem.* **218**, 929–936
- Previato, J. O., Gorin, P. A., Mazurek, M., Xavier, M. T., Fournet, B., Wieruszkes, J. M. and Mendonça-Previato, L. (1990) Primary structure of the oligosaccharide chain of lipopeptidophosphoglycan of epimastigote forms of *Trypanosoma cruzi*. *J. Biol. Chem.* **265**, 2518–2526
- De Lederkremer, R. M., Lima, C. E., Ramirez, M. I., Ferguson, M. A. J. and Thomas-Oates, J. (1991) Complete structure of the glycan of lipopeptidophosphoglycan from *Trypanosoma cruzi* epimastigotes. *J. Biol. Chem.* **266**, 23670–23675

- 20 Bertello, L. E., Gonçalves, M. F., Colli, W. and de Lederkremer, R. M. (1995) Structural analysis of inositol phospholipids from *Trypanosoma cruzi* epimastigote forms. *Biochem. J.* **310**, 255–261
- 21 Bertello, L. E., Andrews, N. W. and de Lederkremer, R. M. (1996) Developmentally regulated expression of ceramide in *Trypanosoma cruzi*. *Mol. Biochem. Parasitol.* **79**, 143–151
- 22 Uhrig, M. L., Couto, A. S., Colli, W. and de Lederkremer, R. M. (1996) Characterization of inositol phospholipids in *Trypanosoma cruzi* trypomastigote forms. *Biochim. Biophys. Acta* **1300**, 233–239
- 23 Agusti, R., Couto, A. S., Campetella, O., Frasch, A. C. C. and de Lederkremer, R. M. (1998) Structure of the glycosylphosphatidylinositol-anchor of the *trans*-sialidase from *Trypanosoma cruzi* metacyclic trypomastigote forms. *Mol. Biochem. Parasitol.* **97**, 123–131
- 24 Sipos, G., Reggiori, F., Vionnet, C. and Conzelmann, A. (1997) Alternative lipid remodeling pathways for GPI membrane anchors in *Saccharomyces cerevisiae*. *EMBO J.* **16**, 3494–3505
- 25 Reggiori, F., Canivenc-Gansel, E. and Conzelmann, A. (1997) Lipid remodeling leads to the introduction and exchange of defined ceramides on GPI proteins in the ER and Golgi of *Saccharomyces cerevisiae*. *EMBO J.* **16**, 3506–3518
- 26 Reggiori, F. and Conzelmann, A. (1998) Biosynthesis of inositol phosphoceramide and remodeling of glycosylphosphatidylinositol anchors in *Saccharomyces cerevisiae* are mediated by different enzymes. *J. Biol. Chem.* **273**, 30550–30559
- 27 Becker, G. W. and Lester, R. L. (1980) Biosynthesis of phosphoinositol-containing sphingolipids from phosphatidylinositol by a membrane preparation from *Saccharomyces cerevisiae*. *J. Bacteriol.* **142**, 747–754
- 28 Dickson, R. C. (1998) Sphingolipid functions in *Saccharomyces cerevisiae*: comparison to mammals. *Annu. Rev. Biochem.* **67**, 27–48
- 29 Ichikawa, S. and Hirabayashi, Y. (1998) Glucosylceramide synthase and glycosphingolipid synthesis. *Trends Cell Biol.* **8**, 198–202
- 30 Dickson, R. C. and Lester, R. L. (1999) Yeast sphingolipids. *Biochim. Biophys. Acta* **1438**, 305–321
- 31 Nagiec, M. M., Nagiec, E. E., Baltisberger, J. A., Wells, G. B., Lester, R. L. and Dickson, R. C. (1997) Sphingolipid synthesis as a target for antifungal drugs. Complementation of the inositol phosphorylceramide synthase defect in a mutant strain of *Saccharomyces cerevisiae* by the *AUR1* gene. *J. Biol. Chem.* **272**, 9809–9817
- 32 Takesako, K., Ikai, K., Haruna, F., Endo, M., Shimanaka, K., Sono, E., Nakamura, T., Kato, I. and Yamaguchi, H. (1991) Aureobasidins, new antifungal antibiotics: taxonomy, fermentation, isolation, and properties. *J. Antibiotics* **44**, 919–924
- 33 Takesako, K., Kuroda, H., Inoue, T., Haruna, F., Yoshikawa, Y., Kato, I., Uchida, K., Hiratani, T. and Yamaguchi, H. (1993) Biological properties of aureobasidin A, a cyclic depsipeptide antifungal antibiotic. *J. Antibiotics* **46**, 1414–1420
- 34 Mandala, S. M., Thornton, R. A., Rosenbach, M., Milligan, J., Garcia-Calvo, M., Bull, H. G. and Kurtz, M. (1997) Khafrefungin, a novel inhibitor of sphingolipid synthesis. *J. Biol. Chem.* **272**, 32709–32714
- 35 Mandala, S. M., Thornton, R. A., Milligan, J., Rosenbach, M., Garcia-Calvo, M., Bull, H. G., Harris, G., Abruzzo, G. K., Flattery, A. M., Gill, C. J. et al. (1998) Rustmicin, a potent antifungal agent, inhibits sphingolipid synthesis at inositol phosphoceramide synthase. *J. Biol. Chem.* **273**, 14942–14949
- 36 Luberto, C., Toffaletti, D. L., Wills, E. A., Tucker, S. C., Casadevall, A., Perfect, J. R., Hannun, Y. A. and Del Poeta, M. (2001) Roles of inositol-phosphoryl ceramide synthase 1 (*IPC1*) in pathogenesis of *C. neoformans*. *Genes Dev.* **15**, 201–212
- 37 Heung, L. J., Luberto, C., Plowden, A., Hannun, Y. A. and Del Poeta, M. (2004) The sphingolipid pathway regulates Pkc1 through the formation of diacylglycerol in *Cryptococcus neoformans*. *J. Biol. Chem.* **279**, 21144–21153
- 38 Previato, J. O., Jones, C., Gonçalves, L. P. B., Wait, R., Travassos, L. R. and Mendonça-Previato, L. (1994) *O*-glycosidically linked *N*-acetylglucosamine-bound oligosaccharides from glycoproteins of *Trypanosoma cruzi*. *Biochem. J.* **301**, 151–159
- 39 Andrews, N. W., Alves, M. J. M., Schumacher, R. I. and Colli, W. (1985) *Trypanosoma cruzi*: protection in mice immunized with 8-methoxypsoralen-inactivated trypomastigotes. *Exp. Parasitol.* **60**, 255–262
- 40 Jacobson, E. S., Ayers, D. J., Harrell, A. C. and Nicholas, C. C. (1982) Genetic and phenotypic characterization of capsule mutants of *Cryptococcus neoformans*. *J. Bacteriol.* **150**, 1292–1296
- 41 Heise, N., Gutierrez, A. L. S., Mattos, K. A., Jones, C., Wait, R., Previato, J. O. and Mendonça-Previato, L. (2002) Molecular analysis of a novel family of complex glycoinositolphosphoryl ceramide from *Cryptococcus neoformans*: structural differences between encapsulated and acapsular yeast forms. *Glycobiology* **12**, 409–420
- 42 Lux, H., Heise, N., Klenner, T., Hart, D. T. and Oppendoerfer, F. R. (2000) Ether-lipid (alkyl-phospholipid) metabolism and the mechanism of action of ether-lipid analogues in *Leishmania*. *Mol. Biochem. Parasitol.* **111**, 1–14
- 43 Saraiva, V. B., Gibaldi, D., Previato, J. O., Mendonça-Previato, L., Bozza, M. T., Freire-de-Lima, C. G. and Heise, N. (2002) Proinflammatory and cytotoxic effects of hexadecylphosphocholine (Miltefosine) against drug-resistant strains of *Trypanosoma cruzi*. *Antimicrob. Agents Chemother.* **46**, 3472–3477
- 44 Kawano, J., Oinuma, T., Nakayama, T. and Sugauma, T. (1992) Characterization of beta 1-4 galactosyltransferase purified from rat liver microsomes. *J. Biochem. (Tokyo)* **111**, 568–572
- 45 Lowry, O. M., Rosebrough, N. J., Farr, A. L. and Randall, R. J. (1951) Protein measurement with the pholin phenol reagent. *J. Biol. Chem.* **193**, 265–275
- 46 Fischl, A. S., Liu, Y., Browdy, A. and Cremesti, A. E. (2000) Inositolphosphoryl ceramide synthase from yeast. *Methods Enzymol.* **311**, 123–130
- 47 Previato, J. O., Sola-Penna, M., Agrellos, O. A., Jones, C., Oeltmann, T., Travassos, L. R. and Mendonça-Previato, L. (1998) Biosynthesis of *O*-*N*-acetyl-glucosamine-linked glycans in *Trypanosoma cruzi*. Characterization of the novel uridine diphospho-*N*-acetylglucosamine:polypeptide *N*-acetylglucosaminyltransferase-catalyzing formation of *N*-acetylglucosamine- α -1-*O*-threonine. *J. Biol. Chem.* **273**, 14982–14988
- 48 Zhong, W., Murphy, D. J. and Georgopapadakou, N. H. (1999) Inhibition of yeast inositol phosphorylceramide synthase by aureobasidin A measured by a fluorometric assay. *FEBS Lett.* **463**, 241–244
- 49 Ikai, K., Takesako, K., Shiomi, K., Moriguchi, M., Umeda, Y., Yamamoto, J. and Kato, I. (1991) Structure of aureobasidin A. *J. Antibiotics* **44**, 925–933
- 50 Kino, K., Taguchi, Y., Komano, T. and Ueda, K. (1996) Aureobasidin A, an antifungal cyclic depsipeptide antibiotic, is a substrate for both human MDR1 and MDR2/P-glycoproteins. *FEBS Lett.* **399**, 29–32
- 51 Tiberghien, F., Kurome, T., Takesako, K., Didier, A., Wenandy, T. and Loor, F. (2000) Aureobasidins: structure-activity relationships for the inhibition of the human MDR1 P-glycoprotein ABC-transporter. *J. Med. Chem.* **43**, 2547–2556
- 52 Zhong, W., Jaffries, M. W. and Georgopapadakou, N. H. (2000) Inhibition of inositol phosphorylceramide synthase by aureobasidin A in *Candida* and *Aspergillus* species. *Antimicrob. Agents Chemother.* **44**, 651–653
- 53 Bromley, P. E., Li, Y. O., Murphy, S. M., Summer, C. M. and Lynch, D. V. (2003) Complex sphingolipid synthesis in plants: characterization of inositolphosphorylceramide synthase activity in bean microsomes. *Arch. Biochem. Biophys.* **417**, 219–226
- 54 Levine, T. P., Wiggins, C. A. R. and Munro, S. (2000) Inositol phosphorylceramide synthase is located in the Golgi apparatus of *Saccharomyces cerevisiae*. *Mol. Biol. Cell* **11**, 2267–2281
- 55 Bertello, L. E., Alves, M. J. M., Colli, W. and de Lederkremer, R. M. (2000) Evidence for phospholipases from *Trypanosoma cruzi* active on PI and IPC. *Biochem. J.* **345**, 77–84
- 56 Sipos, G., Puoti, A. and Conzelmann, A. (1994) GPI membrane anchors in *Saccharomyces cerevisiae*: absence of ceramides from complete precursor glycolipids. *EMBO J.* **13**, 2789–2796
- 57 Furuya, T., Kashuba, C., Docampo, R. and Moreno, S. N. J. (2000) A novel PI-PLC of *Trypanosoma cruzi* that is lipid modified and activated during trypomastigote to amastigote differentiation. *J. Biol. Chem.* **275**, 6428–6438
- 58 Saito, M. L., Furuya, T., Moreno, S. N., Docampo, R. and de Lederkremer, R. M. (2002) The phosphatidylinositol-phospholipase C from *Trypanosoma cruzi* is active on inositolphosphoceramide. *Mol. Biochem. Parasitol.* **119**, 131–133
- 59 Saito, M. L., Bertello, L. E., Vieira, M., Docampo, R., Moreno, S. N. J. and de Lederkremer, R. M. (2003) Formation and remodeling of inositolphosphoceramide during differentiation of *Trypanosoma cruzi* from trypomastigote to amastigote. *Eukaryot. Cell* **2**, 756–768
- 60 Heidler, S. A. and Radding, J. A. (2000) Inositol phosphoryl transferases from human pathogenic fungi. *Biochim. Biophys. Acta* **1500**, 147–152
- 61 Hashida-Okado, T., Ogawa, A., Endo, M., Yasumoto, R., Takesako, K. and Kato, I. (1996) Isolation and characterization of the aureobasidin A-resistant gene *aur1^R*, on *Schizosaccharomyces pombe*: roles of Aur1p in cell morphogenesis. *Mol. Gen. Genet.* **251**, 236–244
- 62 Dickson, R. C. and Lester, R. L. (2002) Sphingolipid functions in *Saccharomyces cerevisiae*. *Biochim. Biophys. Acta* **1583**, 13–25
- 63 Waggoner, D. W., Xu, J., Singh, I., Jasinska, R., Zhang, Q. and Brindley, D. N. (1999) Structural organization of mammalian lipid phosphate phosphatases: implication for signal transduction. *Biochim. Biophys. Acta* **1439**, 199–316
- 64 Hashida-Okado, T., Yasumoto, R., Endo, M., Takesako, K. and Kato, I. (1996) *AUR1*, a novel gene conferring aureobasidin resistance on *Saccharomyces cerevisiae*: a study of defective morphologies in Aur1p-depleted cells. *Curr. Genet.* **33**, 38–45
- 65 Kuroda, M., Hashida-Okado, T., Yasumoto, R., Gomi, K., Kato, I. and Takesako, K. (1999) An aureobasidin A resistance gene isolated from *Aspergillus* is a homolog of yeast *AUR1*, a gene responsible for inositol phosphorylceramide (IPC) synthase activity. *Mol. Gen. Genet.* **261**, 290–296